Title	Gravity-driven microfiltration pretreatment for reverse osmosis (RO) seawater desalination: Microbial community characterization and RO performance
Author(s)	Wu, Bing; Suwarno, Stanislaus Raditya; Tan, Hwee Sin; Kim, Lan Hee; Hochstrasser, Florian; Chong, Tzyy Haur; Burkhardt, Michael; Pronk, Wouter; Fane, Anthony Gordon
Citation	Wu, B., Suwarno, S. R., Tan, H. S., Kim, L. H., Hochstrasser, F., Chong, T. H., et al. (2017). Gravity-driven microfiltration pretreatment for reverse osmosis (RO) seawater desalination: Microbial community characterization and RO performance. Desalination, 418, 1-8.
Date	2017
URL	http://hdl.handle.net/10220/44070
Rights	© 2017 Elsevier. This is the author created version of a work that has been peer reviewed and accepted for publication by Desalination, Elsevier. It incorporates referee's comments but changes resulting from the publishing process, such as copyediting, structural formatting, may not be reflected in this document. The published version is available at: [http://dx.doi.org/10.1016/j.desal.2017.05.024].

Gravity-Driven Microfiltration Pretreatment for Reverse Osmosis (RO) Seawater Desalination: Microbial Community Characterization and RO Performance

Bing Wu[1,*], Stanislaus Raditya Suwarno[1], Hwee Sin Tan[1],

Lan Hee Kim[1], Florian Hochstrasser[2], Tzyy Haur Chong[1,3,*],

Michael Burkhardt[2], Wouter Pronk[4], Anthony G. Fane[1]

1 Singapore Membrane Technology Centre, Nanyang Environment and Water Research Institute, Nanyang Technological University, 1 Cleantech Loop, CleanTech One #06-08, Singapore 637141

2 UMTEC, University of Applied Sciences Rapperswil, Oberseestrasse 10, Switzerland 8640

3 School of Civil and Environmental Engineering, Nanyang Technological University, 50 Nanyang Avenue, Singapore 639798

4 EAWAG, Swiss Federal Institute of Aquatic Science and Technology, Ueberlandstrasse 133, Duebendorf, Switzerland CH-8600

Bing Wu, Email: wubing@ntu.edu.sg

Tzyy Haur Chong, Email: thchong@ntu.edu.sg

Abstract

A pilot gravity-driven microfiltration (GDM) reactor was operated on-site for over 250 days to pretreat seawater for reverse osmosis (RO) desalination. The microbial community analysis indicated that the dominant species in the pilot GDM system (~18.6 L/m^{2}h) were completely different from those in the other tested GDM systems (~2.7-17.2 L/m^{2}h), operating on the same feed. This was possibly due to the differences in available space for eukaryotic movement, hydraulic retention time (i.e., different organic loadings) or operation time (250 days vs. 25-45 days). *Stichotrichia*, *Copepoda*, and *Pterygota* were predominant eukaryotes at genus level in the pilot GDM. Furthermore, the GDM pretreatment led to a significantly lower RO fouling potential in comparison to the UF system. This was attributed to the fact that GDM filtration produced a permeate with less amount of assimilable organic carbon (AOC) and biopolymers. Accordingly, lower amount of organic foulants (biopolymers and low molecular weight neutrals) and less biofilm formation on the GDM-RO membrane were observed. Although α-proteobacteria were dominant in both RO fouling layers, their bacterial community compositions at genus level were significantly different. *Thalassobius* had higher abundance in the GDM-RO fouling layers, while *Erythrobacter and Hyphomonas* were more predominant in the UF-RO fouling layers.

Key words: Assimilable organic carbon; Biofouling; Eukaryotic community; Gravity-driven microfiltration; Prokaryotic community; Seawater pretreatment

1. Introduction

A dual membrane process for seawater desalination, i.e., a low-pressure microfiltration (MF) or ultrafiltration (UF) membrane followed by a reverse osmosis (RO) process, has been developed at full scale since more than twenty years [1]. Compared to conventional seawater pretreatment (such as coagulation-flocculation and media filtration), the membrane-based pretreatment is able to tolerate unfavourable variations in feed seawater, has high removal efficiencies of colloids and suspended particles, and has lower chemical consumption and sludge production. Consequently, the RO membrane system can be operated at a higher permeate flux and lower frequency of chemical cleaning, thus resulting in a decrease of the overall cost of seawater desalination [2-6].

However, a major disadvantage of the membrane-based pretreatment technology is the fouling of the pretreatment membrane itself, which causes productivity decline and higher operational costs. In addition, due to the poor rejection of dissolved organic substances by MF/UF, biofouling of RO membrane may not be effectively alleviated [6]. To improve the pretreatment performance, integration of low-pressure membrane processes with other processes has received increasing attention. Coagulation, ion-exchange, and adsorption technologies have been successfully combined with membrane-based pretreatment to mitigate fouling and improve the permeate quality [2, 3]. Furthermore, a hybrid process that integrates biological treatment and coagulation/adsorption with a low-pressure membrane (i.e., membrane bioreactor) has also been proposed, in which the dissolved organic substances could be biologically degraded and physically coagulated/adsorbed due to the longer seawater retention time in the bioreactor [7-9].

Alternatively, gravity-driven membrane (GDM) filtration has been proven to be effective in pretreating seawater as a chemical free and low energy option [10-12], in which the rejected

organic substances are biodegraded by the biofilm on the membrane. In our previous study [12], a pilot submerged GDM reactor was successfully operated for more than 250 days without any physical and chemical cleaning (the stabilized flux of ~ 18.6 L/m^{2}h; the operation of the pilot system is ongoing and almost 450 days at the time of writing this paper). In particular, the biofilm in the pilot GDM reactor facilitated the reduction in assimilable organic carbon (AOC) and biopolymers. It has been reported that the biopolymers would lead to a conditioning layer that initiate the biofilm development as well as organic fouling [13, 14], while AOC level (fraction of "labile" or "bio-available" DOC) in RO feed water was found to be positively correlated with the biofouling of RO systems [15-17].

On the other hand, the moving, grazing and sloughing behaviours of eukaryotic organisms within the fouling layer played a dominant role in controlling the morphology of fouling layer, which in turn had great impact on the stabilized flux. Previous studies [18-20] on surface water treatment by GDM systems showed that protists (such as flagellates, ciliates, amoebae, and heliozoans), and metazoa (such as rotifer, nematodes, and oligochaetes) were the major contributors to enhance the formation of heterogeneous fouling layer on the membranes. We proposed that the advantages of the longer residence time of organic substances and the availability of sufficient space for the growth, predation, and movement of the eukaryotes in the pilot GDM reactors were responsible for the higher flux and better degradation of organics in the submerged systems [12].

To further illustrate the microbial behaviors in the GDM system and to evaluate the feasibility of GDM pretreatement for RO seawater desalination, in this study, we aim to (1) identify the dominant prokaryotes and eukaryotes in the pilot GDM reactor, lab GDM reactor, and filtration cell system; (2) compare the performances of RO membranes fed with the pilot GDM permeate and full-scale UF permeate; (3) characterize the organic and

microbial community compositions of the fouling layer extracted from the RO membranes. This study allows us to understand better the transportation pathway of organic substances in the GDM-RO system and to provide meaningful insights for further scale-up of the system.

2. Materials and Methods

2.1. Seawater feed

Seawater was collected from the R&D site next to a full scale desalination plant in Singapore. As seawater was chlorinated at the intake before it was delivered to the collection tank, de-chlorination was performed before use. A certain amount of sodium bisulphite (Acros Organics, USA) was added into the feed tank to ensure the total chlorine concentration was zero (measured by a colorimeter, Thermo Fisher scientific, USA).

2.2. GDM setup

A pilot-scale GDM reactor (effective volume of 720 L, operation for 250 days, hydraulic retention time (HRT) of 21.6 h) was set up at the R&D site next to a full scale desalination plant in Singapore. A flat sheet microfiltration (MF) membrane (PVDF, 0.08 μm) module was submerged into the reactor and the module was located 40 cm below the water level of the overflow line (i.e., a hydrostatic pressure of 0.04 bar). The room temperature was at 26±1°C. A lab-scale GDM reactor (effective volume of 8.4 L, operation for 45 days, HRT of 13 h) and a GDM filtration cell system (feed side volume of 0.0046 L, operation for 45 days, HRT of 0.74 h) were operated at the same hydrostatic pressure at 0.04 bar using the same flat sheet membrane (PVDF, 0.08 μm). The room temperature was 21±1°C. The details of each setup were described previously [12] and are summarized in Table S1.

The permeate flux (L/m^2h) was obtained by dividing the volume of permeate collected during a given period of filtration by the membrane area. The permeate flux was normalized to a

115 temperature of 27°C (yearly mean atmosphere temperature in Singapore) as described
116 previously [12].

117 *2.3. RO setup*

118 Two parallel stainless steel RO cells with commercial RO membrane (DOW FilmTec, model
119 BW-30) were set up at the pilot plant. The pilot GDM permeate and the UF (PES, 120 kDa)
120 permeate from the co-located full scale desalination plant were collected as the RO feed
121 respectively. In each RO unit, a stirrer (IKA, Germany) and chiller were installed inside of
122 the feed tank (10 L) in order to maintain a constant temperature of 26±1°C. A high-pressure
123 pump (HydraCell, USA) was employed to deliver the feed water to the RO cell at a constant
124 crossflow velocity at 0.17 m/s. The two RO systems were operated at the same permeate flux
125 of 20 L/m^2 h and their respective permeate flowrate was regulated by a mass flow controller
126 (Brooks Instrument, USA). The conductivities of feed and permeate were measured by
127 conductivity meters (Thermo Scientific, USA). In this study, the RO concentrate and RO
128 permeate were recirculated to feed tank and the test solution in the feed tanks was replenished
129 daily. A computer equipped with data logging system (LabVIEW, National Instruments, USA)
130 was used to continuously record the pressure, flowrate, and conductivity in both RO systems
131 [21, 22]. The transmembrane pressure (TMP) was calculated based on the difference between
132 the feed and permeate pressure. The ratio of TMP/TMP$_0$ was used to describe the RO
133 membrane fouling development, in which TMP$_0$ represents the initial TMP.

134 *2.4. Water quality parameters*

135 The dissolved organic carbon (DOC) of water sample was monitored using a TOC analyzer
136 (Shimadzu, Japan) after being filtered through a 0.45 μm hydrophilic filter. The turbidity of
137 the seawater was examined using a turbidity meter (Hach, US). The bacterial amount in the
138 permeate was measured by a flow cytometry (BD Biosciences, US).

139 *2.5. Transparent exopolymer particles (TEP) measurement*

140 The TEP in the permeate was examined after the permeate sample was filtered through a
141 polycarbonate filter (Millipore, USA; a pore size of 0.1 μm). Three mL of 0.02% aqueous
142 solution of alcian blue in 0.06% acetic acid (Aldrich-Sigma, USA) was used to stain the
143 retained TEP on the filter. The excess dye was then removed by distilled water. The filter
144 with stained TEP was put into a beaker with 6 mL of 80% H_2SO_4 solution (Honeywell,
145 Korea) and the solution was collected after 2 hr. The absorption of the solution was measured
146 at a wavelength of 787 nm using a spectrometer (Hach, USA) and the concentration of TEP
147 was calculated based on a calibration curve with gum xanthan (Sigma-Aldrich, USA) as a
148 TEP standard [23, 24].

149 *2.6. Liquid chromatography-organic carbon detection-organic nitrogen detection (LC-OCD-*
150 *OND)*

151 To quantify the soluble organic fractions (<0.45 μm, e.g., biopolymers, humics, building
152 blocks, low molecular weight neutrals and acids) in the feed, permeate, and soluble foulants,
153 size-exclusion chromatography integrated with organic carbon detection and organic nitrogen
154 detection was used. The mobile phase (1.1 mL/min) was delivered by an HPLC pump
155 (Knauer, Germany) to an autosampler (MLE, Germany) and the chromatographic column
156 (Toso, Japan). A UV-detector (at a wavelength of 254 nm, Knauer, Germany) was employed
157 to analyze organic carbon. A variable wavelength UV-detector (220 nm, 254 nm, 280 nm and
158 350 nm, Knauer, Germany) and a Deuterium lamp is used for Organic Nitrogen Detection
159 [25].

160 *2.7. Assimilable organic carbon (AOC) examination*

The assimilable organic carbon (AOC) measurement was performed based on the methods described by Hammes et al. [26]. The permeate samples were filtered with a 0.22 μm membrane filter (Millipore, USA) and the filtrate was collected using a 40 ml vial with PTFE covers (Thermo Scientific, USA). After the sample was sterilized in a water bath at 70 °C for 30 min, it was inoculated with raw seawater. After 72 h of incubation at 30°C, 1 ml of sample and 10 μl of 0.2 M EDTA (Kanto Chemical, Japan) were mixed and incubated at 37°C for 10 min. The sample was stained with 10 μl of SYBR green (Molecular Probes, USA) at a concentration of 100×. After incubation at 37°C for 20 min, the stained sample and unstained sample (as a control) were transferred to a flat bottom well plate for flow cytometry analysis. AOC concentration was calculated based on the cell counts in a defined region of a density plot according to the standard curve (94164 cells/L equivalent to 1 μg AOC as acetate/L).

2.8. Confocal laser scanning microscopy (CLSM) observation

The LIVE/DEAD® BacLight™ Bacterial Viability kit (Invitrogen, USA) was used to stain the fouled RO membranes following the manufacturer's protocols. The morphology of the biofilm was observed and recorded by a CLSM (×10 objective, ZEISS, Germany). The biovolumes (μm^3/membrane area μm^2) of the biofilm were obtained from the images using IMARIS software (Bitplane, Switzerland) [21].

2.9. Adenosine tri-phosphate (ATP) analysis

The microbial activity was determined by measuring the ATP concentration of total microbes in the foulants. ATP was measured using the Kikkoman's ATP assay kit and a luminometer (Lumitester C-110, Kikkoman, Japan) according to the manufacturer's protocols.

2.10. Microbial community analysis

184 The biofilm samples were collected from the fouled GDM and RO membrane surfaces and
185 the settled sludge was collected from the bottom of the pilot reactor. The genomic DNA of
186 the microbial community in the samples was extracted by FastDNA® SPIN kit (MP
187 Biomedicals, USA). The 16S/18S rRNA gene was sequenced by Illumina (Research and
188 Testing Laboratory, USA) using primers 357wF (CCTACGGGNGGCWGCAG) and 785R
189 (GACTACHVGGGTATCTAATCC) for prokaryotes, TAReukF
190 (CCAGCASCYGCGGTAATTCC) and TAReukR (ACTTTCGTTCTTGATYRA) for
191 eukaryotes. The sequencing results were analysed by Mothur 1.35.1 software [27] using the
192 standard de novo operational taxonomic unit (OTU)-based approach.

193 **3. Results and Discussion**

194 *3.1. Effect of GDM configuration on microbial community composition*

195 In the pilot GDM reactor, lab GDM reactor, GDM filtration cell, and submerged GDM
196 filtration cell in the lab reactor, the biofouling layers were carefully collected from the
197 membrane surfaces at day 250, 45, 45, and 25, respectively (i.e., at the end of operation,
198 except for the pilot GDM reactor which is ongoing at the time of writing). The prokaryotic
199 and eukaryotic (only for the pilot GDM reactor) community diversities were cataloged by
200 sequencing 16S rRNA and 18S rRNA genes respectively. The prokaryotic community
201 structures at various taxonomic levels (phylum, class, and genus) are shown in Figure 1. It
202 was found that more than 98% of bacterial sequences were related to twelve different phyla
203 for the four GDM systems tested, such as Acidobacteria, Actinobacteria, Bacteroidetes,
204 Chlamydiae, Chloroflexi, Cyanobacteria, Firmicutes, Gemmatimonadetes, Nitrospirae,
205 Planctomycetes, Proteobacteria, Verrucomicrobia. Proteobacteria showed the highest
206 abundance (53-89%) in the biofouling layer, regardless of the GDM configuration.

At class level, both α-Proteobacteria (40-69%, especially Rhodobacteraceae family) and γ-Proteobacteria (8-17%), were predominant in the biofouling layers of the four GDM systems. Especially, the abundances of α- and γ-Proteobacteria in the biofilms (69% and 17% respectively) of the GDM filtration cell were significantly higher than those of the pilot and lab GDM reactors as well as the GDM filtration cell submerged into the lab reactor (40-55% and 2-7% respectively). Previous studies have pointed out that α- and γ-Proteobacteria are dominant components in the intake seawater [28] as well as being responsible for the major pioneering activity formation of biofilms on the membrane in pretreating seawater [29]. On the other hand, in the previous study [12], very limited numbers of eukaryotes were found in the GDM filtration cell, while a more diverse and higher amount of eukaryotes were observed in the pilot GDM reactor. Because the eukaryotic sizes ranged from around 100 μm to a few millimeters [12], the limited space of the GDM filtration cell may not be suitable for the eukaryotic proliferation. As a result of more biofilm-forming species and low eukaryote activity, the GDM filtration cell achieved a lower permeate flux (2.7±0.6 L/m^2h) compared to the other GDM systems (16.3-18.6 L/m^2h).

In addition, greater amounts of Actinobacteria, Bacilli, Gemmatimonadetes, Nitrospira, Planctomycetacia, Candidatus_Thiobios, and δ-Proteobacteria were attached on the membrane in the pilot GDM reactor than those in the lab GDM reactor and GDM filtration cells. It should be noted that the pilot GDM reactor had been in operation for 250-day at a HRT of 21.6 h, which was much longer than the lab GDM reactor (45 days; HRT of 13 h), the filtration cell submerged into the lab reactor (25 days; HRT of 13 h) and the filtration cell (45 days; HRT of 0.74 h). Possibly, these bacteria were prone to grow at relatively lower organic loading (i.e., longer HRT) and their growth was faster than the reduction by eukaryotic predation. Accordingly, with extending operation time, their abundance increased in the pilot GDM reactor.

232 At the genus level, the microbial communities in the biofouling layers of the GDM systems
233 were highly diversified and composed of more than 300 OTUs, but in total only 51 species
234 were present at abundance higher than 1%. Obviously, *Roseobacter* clade, which fall within
235 the α subdivision of the division Proteobacteria was predominant in the four GDM systems
236 tested. This is not surprising as *Roseobacter* clade is one of the major groups in marine
237 bacterioplankton communities [30]. In particular, *Roseobacter* clade had a significantly
238 higher abundance in the biofouling layer of GDM filtration cell (28%) than those in the GDM
239 reactors and GDM filtration cell that was submerged into the reactor (5-10%). This genus has
240 been found to be in commensal relationships with marine phytoplankton, invertebrates, and
241 vertebrates [30]. Thus, their lower abundance may be attributed to the predation activity of
242 the eukaryotes in the GDM reactors, which were suitable for the proliferation of eukaryotes.
243 In addition, *Hyphomonas*, *Citreimonas*, *Pseudoruegeria*, and *Methylophaga* in the biofouling
244 layer of GDM filtration cell (5.2%, 3.9%, 3.9%, and 5.5% respectively) had slightly higher
245 abundance than in the other GDM systems (0.4-4.3%, <0.1%, 0.6-1.1%, and <0.3%
246 respectively). Such bacterial species would also be a favourable prey for the eukaryotes
247 growing in the GDM reactor.

248 It has been well illustrated previously that the movement and predation behaviour of
249 eukaryotic organisms in the biofouling layer would determine the morphology of the
250 biofouling layer, which in turn has an impact on the stabilized membrane permeate flux [12,
251 18, 20]. Figure 2 shows the eukaryotic compositions of settled sludge (which peeled off from
252 the membrane surface) and biofouling layer in the pilot GDM reactor. Apparently, more
253 diverse eukaryotes were noticed in the biofouling layer than in the settled sludge. This
254 illustrates that the attached-growing bacterial matrix on the membrane provides favorable
255 scenarios for the growth, movement, and predation activities of eukaryotes.

In detail, Metazoa was the major eukaryote phylum in the pilot GDM reactor, accounted for 96% and 57% in the settled sludge and biofouling layer, respectively. In addition, the abundance of other phyla, such as Alveolata, Fungi, Viridiplantae, and Stramenopiles, was higher in the biofouling layer than in the settled sludge. At class level, Arthropoda was predominant in the Metazoa phylum (90% in the settle sludge and 49% in the biofouling layer). Ciliophora was the second major eukaryote group in the biofouling layer, accounting for 21%. At genus level, *Stichotrichia* (15%), *Copepoda* (25%), and *Pterygota* (18%) were the predominant species derived from the biofouling layer, while only *Copepoda* (86%) was the dominant species in the settled sludge.

3.2. Effect of GDM pretreatment on RO performance

3.2.1. RO feed water characteristics

The characteristics of the pilot GDM permeate and the full-scale UF permeate are listed in Table 1. Both pretreatment processes produced superior permeate turbidity (i.e., NTU value almost ~0, data not shown) due to membrane rejection of all particulate and colloidal matters. Recent studies indicate that TEP could potentially cause particulate/colloidal and biological fouling in RO membrane processes because they are mainly composed of surface-active acidic polysaccharides [31]. It is evident that the UF pretreatment produced permeate with less TEP (i.e., solute size greater than 0.1 μm) than the GDM pretreatment. The MF membrane (0.08 μm) used in the pilot GDM reactor had relatively larger pore size than the UF membrane (~ 120kDa) used in the full scale plant, which could not retain the colloidal TEP and TEP precursors. However, the bacterial amount in both permeates were relatively indifferent because most of the bacterial cells were larger than the membrane pore size of MF and UF.

279 Comparable DOC contents (1.29±0.33 vs. 1.21±0.13 mg/L) were found in both permeates, in
280 which about 76-79% of DOC compounds were humics and low molecular weight (LMW)
281 neutrals. This observation was in agreement with the findings in other studies using LC-OCD
282 for seawater organics characterization that humics and LMW neutrals were the main
283 components [16, 17, 32]. In detail, less biopolymers (>10 kDa) were present in the pilot
284 GDM permeate, while less LMW neutrals in the UF permeate were noticed. The biopolymers
285 are generally composed of polysaccharides and also contain nitrogen-containing substances
286 such as proteins or amino sugars. LMW neutrals refer to the fraction with low molecular
287 weight (<350 Da) and low ion density, such as alcohols, aldehydes, ketones, sugars, and
288 amino acids [25]. Due to the size exclusion effect, the UF membranes (~120 kDa) should be
289 more effective in retaining the biopolymers than the MF membrane (0.08 μm) used in the
290 pilot GDM reactor; while has a comparable LMW neutrals rejection efficiency to the MF
291 membrane as in principle both membranes are not able to retain LMW neutrals. In this study,
292 real seawater was used, in which diverse bacteria were existing. Therefore, this phenomenon
293 may be associated with the fact that the bacterial community in the pilot GDM reactor
294 potentially degraded the biopolymers to LMW neutrals, leading to less biopolymers and more
295 LMW neutrals than in the UF system. In addition, there was almost no significant difference
296 in the amount of humics (~1 kDa) and building blocks (300-500 Da, reflecting the breakdown
297 products of humic substances) in both permeates, possibly because of similar rejection rates
298 by both UF and MF membranes (i.e., in principle both membranes are not able to retain MW
299 < 1 kDa) and the fact that the biodegradation of humics can be assumed to be negligible.

300 Previous study of the production and molecular weight distribution of TEP/TEP precursors of
301 pure bacteria culture illustrated that TEP/TEP precursors were mainly comprised of
302 biopolymers with a high protein portion, but whether the building blocks and LMW neutrals
303 are also TEP precursors wase not confirmed [14]. In this study, higher concentrations of TEP,

lower concentrations of biopolymers, and higher concentrations of LMW neutrals were present in the pilot GDM permeate than in the UF permeate. It appears that the TEP contents were not related well with the amounts of the biopolymers. This may be related to the following phenomena: (1) the protein-like biopolymers in the pilot GDM permeate may be higher than in the UF permeate, and (2) the LMW neutrals that had smaller size than that of the TEP test membrane may have strong affinity with the filter used in the TEP measurement, thus resulting in the retention of LMW neutrals and subsequently detection as TEP precursors.

The AOC levels in the permeates were monitored to evaluate the amount of bioavailable organics. In this study, the AOC level in the pilot GDM permeate was almost 3-time lower than that in the UF permeate (Table 1). Researchers have found that the quantity of AOC in seawater could be directly correlated to the amount of LMW neutrals of measured by LC-OCD [17, 33]. However, in this study, the concentration of LMW neutrals in the GDM permeate was notably more than in the UF permeate, which did not show the relationship between AOC and LMW neutrals. A possible explanation for this disagreement can be attributed to the different AOC measurement protocols in the reported studies (using *Vibrio fischeri* MJ-1 strain and bioluminescence method [34]) and this study (using mix-culture from seawater and flow cytometry method). As there is lack of a standard AOC measurement protocol for seawater, future studies to focus on the contributions of different organic fractions in seawater towards the AOC content need to be performed.

3.2.2. RO performance

After about 150-days operation of the pilot GDM reactor, the permeate was collected and fed to the RO system to study the effect of pretreatment on RO performance; where UF permeate from the full scale plant was used as baseline for comparison. The TMP/TMP_0 profile is

shown in Figure 3. Periodic fluctuations of TMP/TMP_0 data were noticed, which were linked to the temperature variations of the feed water (the feed water tanks were located outdoor) during day and night.

At the early stage (day 0-1), both GDM-RO and UF-RO showed a similar increase in TMP/TMP_0. The intial increase in resistance was presumably due the interaction of organic substances with the RO membrane, which led to the formation of a conditioning layer on the RO membrane; especially owing to the sticky nature of TEP that facilitates the instantaneous adsoprtion onto the membrane surface [13, 14]. As the conditioning process typically takes several days and the biofilm is only initiated after the conditioning layer is in place [14], fluctuation and insignificant increases in TMP/TMP_0 were noticed during day 1-4 for both GDM-RO and UF-RO.

After day 4, a rapid rise in TMP/TMP_0 was observed in UF-RO, while the TMP/TMP_0 remained relatively constant in the GDM-RO. The higher level of AOC in the UF permeate promoted the greater formation of biofilm on the RO membrane that resulted in the build up of hydraulic resistance. Meanwhile, the heterogeneous structure of the biofilm could hinder back diffusion of solutes through its tortuous path, inducing an enhanced osmotic pressure (i.e., biofilm enhanced osmotic pressure (BEOP) effect) [35]. On the other hand, due to limited availability of AOC (in the GDM-RO), the biofilm layer on the RO membrane was relatively thin and below a threshold level as such the pressure measurement was not sensitive enough for detection of such early fouling [9]. Importantly, these observations imply that the GDM reactor as pretreatment was more effective in alleviating the RO biofouling.

3.2.3. Characteristics of foulants on RO membranes

After 10 day of RO operation, the RO membranes were taken from the setup and the foulants were extracted from the membranes by mild sonication (5-min). The foulant solutions were collected for analysis. Figure S1 shows the CLSM images of the fouled RO membranes and Table 2 describes the biological and organic characteristics of RO membrane foulants. Bioactivity in the RO membrane foulants was evaluated in terms of biovolume of live cells and ATP [9]. Clearly, the biovolume of live cells was detected by the CLSM in the UF-RO foulants ($(6.70\pm0.99)\times10^7$ $\mu m^3/cm^2$) was almost 3-time of that in the GDM-RO foulants ($(2.65\pm0.19)\times10^7$ $\mu m^3/cm^2$). The corresponding ATP level was also greater (6.47 ± 0.67 vs. 2.18 ± 0.19 ng/cm^2). Moreover, the ratio of biovolume of dead cell to total biovolume in the UF-RO foulants (32%) was much greater than in the GDM-RO foulants (18%). It should be noted that both GDM-RO and UF-RO had similar bacterial counts in the feed water, but UF-RO had greater amounts of AOC. Thus, our study was in agreement with previous studies that AOC promoted bacterial proliferation and was a crucial contributor to RO biofouling [15, 36].

Although both UF-RO and GDM-RO had comparable DOC in the feed water, the amount of DOC in the UF-RO foulants was 2.22 ± 0.56 $\mu g/cm^2$, 2-time higher than in the GDM-RO foulants (0.96 ± 0.19 $\mu g/cm^2$). This signifies a reasonable relationship between the nutrient accumulation on the membrane surface due to concentration polarization and the RO fouling rate due to biofilm growth, which was well explained in the previous study [37]. LMW neutrals were the predominant organic components in both RO foulants, accounting for 47-55% of the DOC. Compared to the UF-RO foulants, smaller amounts of biopolymers (~40% lower) and LMW neutrals (~63% lower) were found in the GDM-RO foulants. However, the building blocks contents in both foulants were relatively similar and no humics or LMW acids were detected despite large amounts of humics being present in the feed water (Table 1).

376 The contribution ratios of each organic fractions towards the DOC in GDM permeate, GDM-
377 RO foulants, UF permeate and UF-RO foulants are compared and presented in Figure 4. The
378 higher ratios of biopolymers and LMW neutrals in the RO foulants than in the permeates in
379 both GDM-RO and UF-RO systems imply (1) the accumulation of these components from
380 the feed water in the RO fouling layers; (2) the utilization of LMW neutrals by
381 microorganism in the RO fouling layer and subsequent production of extracellular polymeric
382 substances (i.e., biopolymers) and LMW neutrals during their proliferation. The results
383 suggest that biopolymers and LMW neutrals are potential organic foulants inducing RO
384 fouling in both systems. In some previous reports, the major organics in the RO foulants were
385 inconsistent, possibly due to the difference in pretreatment approaches used and operating
386 duration. For example, humics constituted a major portion of organic fouling of a full-scale
387 RO plant (operation for 8 years) receiving conventional pretreated seawater [16], whereas
388 protein-like substances were identified as major foulants of RO membrane fed with pretreated
389 seawater by hybrid coagulation/adsorption-membrane systems (operation for 45 h) [9].

390 Overall, the analysis of RO foulants illustrated that the higher RO fouling rate in the UF-RO
391 system was possibly attributed to higher biofouling potential (i.e., greater AOC) in the feed
392 water, which resulted in faster biofilm development (i.e., higher viable cells and ATP) and
393 more accumulation of organic substances (especially biopolymers and LMW neutrals) in the
394 fouling layers.

395 *3.2.4. Characteristics of microbial community in RO foulants*

396 The 16S rRNA sequence analysis was utilized to illustrate the effect of pretreatment on
397 bacterial diversity in the RO foulants (Figure 5). The sequencing results indicated that at
398 phylum level, Proteobacteria accounted for more than 93% of total bacteria (Figure 5a), in
399 which α-Proteobacteria was predominant (>82%) in the foulants in both GDM-RO and UF-

RO (Figure 5b). It appeared that the pretreatment approach had negligible effect on the microbial community composition at phylum and class levels.

At genus level, the bacterial community was composed of more than 200 OTUs genus. Most of the OTUs were detected at very low abundance and the species present at a higher abundance than 1% are shown in Figure 5c. Interestingly, the dominant species in the RO foulants were not identical for the GDM and UF pretreatment processes. In the GDM-RO system, *Thalassobius* (44-60%) were the major bacteria proliferating on the RO membrane, while *Hyphomonas* (32%) and *Erythrobacter* (36%) were the predominant bacteria causing RO biofouling in the UF-RO system. This difference may be associated with the available substrates (i.e., AOC) in GDM and UF permeate. Nevertheless, these prevalent bacteria were commonly observed in previous studies. *Thalassobius* is a genus of the Rhodobacteraceae, which was reported as prevalent family in the seawater and on the fouled SWRO membranes [28, 38]. *Hyphomonas* belongs to Hyphomonadaceae family, Caulobacterales order, which plays an important role in biofilm formation by production of different types of extracellular polymeric substances, contributing to adhesion to surfaces and as a biofilm matrix [39]. *Erythrobacter* is known as aerobic phototrophs and represents a separate branch within Erythrobacteraceae family, Sphingomonadales order, which is often found in organic-rich environments and tends to form irregular shaped natural "clumps" [40, 41].

5. Conclusions

In this study, we identified the microbial community compositions of different GDM systems (pilot-scale, lab-scale, and filtration cell) and illustrated the effect of pretreatment (GDM vs. UF) on RO performance and characteristics of RO foulants in the seawater desalination process. The following conclusions can be drawn:

(1) In the tested GDM systems, α-proteobacteria was dominant, but the prokaryotic community composition at genus level was significantly influenced by GDM configuration.

(2) In the pilot GDM reactor, *Stichotrichia*, *Copepoda*, and *Pterygota* were the major eukaryotes with a relatively high abundance.

(3) Compared to the UF pretreatment, the GDM reactor was more effective in removing the biopolymers and AOC, which led to lower organic fouling and biofouling of the RO membrane.

(4) Biopolymers and LMW neutrals were identified as major RO foulants in both UF-RO and GDM-RO systems.

(5) α-Proteobacteria had the highest abundance in both UF-RO and GDM-RO foulants. At genus level, the dominant species in the RO foulants were affected by the pretreatment technique.

Acknowledgements

This study is under Singapore Membrane Technology Centre Seawater Facility project (TBD-WTTM-1504-0002), which is supported by the Public Utilities Board (PUB), Singapore. The Economic Development Board (EDB) of Singapore is acknowledged for funding the Singapore Membrane Technology Centre (SMTC), Nanyang Technological University.

References

[1] M. Busch, R. Chu, S. Rosenberg, Novel trends in dual membrane systems for seawater desalination: minimum primary pretreatment and low environmental impact treatment schemes, IDA J. Desalin. Water Reuse, 2 (2010) 56-71.

[2] L.F. Greenlee, D.F. Lawler, B.D. Freeman, B. Marrot, P. Moulin, Reverse osmosis desalination: Water sources, technology, and today's challenges, Water Res., 43 (2009) 2317-2348.
[3] W.L. Ang, A.W. Mohammad, N. Hilal, C.P. Leo, A review on the applicability of integrated/hybrid membrane processes in water treatment and desalination plants, Desalination, 363 (2015) 2-18.
[4] S. Jamaly, N.N. Darwish, I. Ahmed, S.W. Hasan, A short review on reverse osmosis pretreatment technologies, Desalination, 354 (2014) 30-38.
[5] C.V. Vedavyasan, Pretreatment trends - an overview, Desalination, 203 (2007) 296-299.
[6] N. Voutchkov, Considerations for selection of seawater filtration pretreatment system, Desalination, 261 (2010) 354-364.
[7] S. Jeong, G. Naidu, S. Vigneswaran, Submerged membrane adsorption bioreactor as a pretreatment in seawater desalination for biofouling control, Bioresource Technol., 141 (2013) 57-64.
[8] S. Jeong, S.A. Rice, S. Vigneswaran, Long-term effect on membrane fouling in a new membrane bioreactor as a pretreatment to seawater desalination, Bioresource Technol., 165 (2014) 60-68.
[9] S. Jeong, S.J. Kim, C.M. Kim, S. Vigneswaran, T.V. Nguyen, H.K. Shon, J. Kandasamy, I.S. Kim, A detailed organic matter characterization of pretreated seawater using low pressure microfiltration hybrid systems, J. Membrane Sci., 428 (2013) 290-300.
[10] E. Akhondi, B. Wu, S.Y. Sun, B. Marxer, W.K. Lim, J. Gu, L.B. Liu, M. Burkhardt, D. McDougald, W. Pronk, A.G. Fane, Gravity-driven membrane filtration as pretreatment for seawater reverse osmosis: Linking biofouling layer morphology with flux stabilization, Water Res., 70 (2015) 158-173.
[11] B. Wu, F. Hochstrasser, E. Akhondi, N. Ambauen, L. Tschirren, M. Burkhardt, A.G. Fane, W. Pronk, Optimization of gravity-driven membrane (GDM) filtration process for seawater pretreatment, Water Res., 93 (2016) 133-140.
[12] B. Wu, T. Christen, H.S. Tan, F. Hochstrasser, S.R. Suwarno, X. Liu, T.H. Chong, M. Burkhardt, W. Pronk, A.G. Fane, Improved performance of Gravity-Driven Membrane Filtration for Seawater Pretreatment: Implications of Membrane Module Configuration, Water Res., 114 (2017) 59-68.
[13] T. Berman, R. Mizrahi, C.G. Dosoretz, Transparent exopolymer particles (TEP): A critical factor in aquatic biofilm initiation and fouling on filtration membranes, Desalination, 276 (2011) 184-190.
[14] S. Li, H. Winters, S. Jeong, A.H. Emwas, S. Vigneswaran, G.L. Amy, Marine bacterial transparent exopolymer particles (TEP) and TEP precursors: Characterization and RO fouling potential, Desalination, 379 (2016) 68-74.
[15] L. Weinrich, M. LeChevallier, C.N. Haas, Contribution of assimilable organic carbon to biological fouling in seawater reverse osmosis membrane treatment, Water Res., 101 (2016) 203-213.
[16] S. Jeong, G. Naidu, R. Vollprecht, T. Leiknes, S. Vigneswaran, In-depth analyses of organic matters in a full-scale seawater desalination plant and an autopsy of reverse osmosis membrane, Sep. Purif. Technol., 162 (2016) 171-179.
[17] S. Jeong, R. Vollprecht, K. Cho, T. Leiknes, S. Vigneswaran, H. Bae, S. Lee, Advanced organic and biological analysis of dual media filtration used as a pretreatment in a full-scale seawater desalination plant, Desalination, 385 (2016) 83-92.
[18] N. Derlon, M. Peter-Varbanets, A. Scheidegger, W. Pronk, E. Morgenroth, Predation influences the structure of biofilm developed on ultrafiltration membranes, Water Res, 46 (2012) 3323-3333.

[19] N. Derlon, N. Koch, B. Eugster, T. Posch, J. Pernthaler, W. Pronk, E. Morgenroth, Activity of metazoa governs biofilm structure formation and enhances permeate flux during Gravity-Driven Membrane (GDM) filtration, Water Res, 47 (2013) 2085-2095.
[20] T. Klein, D. Zihlmann, N. Derlon, C. Isaacson, I. Szivak, D.G. Weissbrodt, W. Pronk, Biological control of biofilms on membranes by metazoans, Water Res., 88 (2016) 20-29.
[21] S.R. Suwarno, X. Chen, T.H. Chong, V.L. Puspitasari, D. McDougald, Y. Cohen, S.A. Rice, A.G. Fane, The impact of flux and spacers on biofilm development on reverse osmosis membranes, J. Membrane Sci., 405 (2012) 219-232.
[22] B. Wu, T. Kitade, T.H. Chong, T. Uemura, A.G. Fane, Impact of membrane bioreactor operating conditions on fouling behavior of reverse osmosis membranes in MBR-RO processes, Desalination, 311 (2013) 37-45.
[23] U. Passow, A.L. Alldredge, A dye-binding assay for the spectrophotometric measurement of transparent exopolymer particles (TEP), Limnol. Oceanogr., 40 (1995) 1326-1335.
[24] B. Wu, T. Kitade, T.H. Chong, T. Uemura, A.G. Fane, Role of initially formed cake layers on limiting membrane fouling in membrane bioreactors, Bioresource Technol., 118 (2012) 589-593.
[25] S.A. Huber, A. Balz, M. Abert, W. Pronk, Characterisation of aquatic humic and non-humic matter with size-exclusion chromatography - organic carbon detection - organic nitrogen detection (LC-OCD-OND), Water Res., 45 (2011) 879-885.
[26] F.A. Hammes, T. Egli, New method for assimilable organic carbon determination using flow-cytometric enumeration and a natural microbial consortium as inoculum, Environ. Sci. Technol., 39 (2005) 3289-3294.
[27] P.D. Schloss, S.L. Westcott, T. Ryabin, J.R. Hall, M. Hartmann, E.B. Hollister, R.A. Lesniewski, B.B. Oakley, D.H. Parks, C.J. Robinson, J.W. Sahl, B. Stres, G.G. Thallinger, D.J. Van Horn, C.F. Weber, Introducing mothur: Open-Source, Platform-Independent, Community-Supported Software for Describing and Comparing Microbial Communities, Appl. Environ. Microb., 75 (2009) 7537-7541.
[28] M.L. Zhang, S. Jiang, D. Tanuwidjaja, N. Voutchkov, E.M.V. Hoek, B.L. Cai, Composition and Variability of Biofouling Organisms in Seawater Reverse Osmosis Desalination Plants, Appl. Environ. Microb., 77 (2011) 4390-4398.
[29] H. Bae, H. Kim, S. Jeong, S. Lee, Changes in the relative abundance of biofilm-forming bacteria by conventional sand-filtration and microfiltration as pretreatments for seawater reverse osmosis desalination, Desalination, 273 (2011) 258-266.
[30] A. Buchan, J.M. Gonzalez, M.A. Moran, Overview of the marine Roseobacter lineage, Appl. Environ. Microb., 71 (2005) 5665-5677.
[31] S.J. Meng, M. Rzechowicz, H. Winters, A.G. Fane, Y. Liu, Transparent exopolymer particles (TEP) and their potential effect on membrane biofouling, Appl. Microbiol. Biot., 97 (2013) 5705-5710.
[32] F.X. Simon, Y. Penru, A.R. Guastalli, S. Esplugas, J. Llorens, S. Baig, NOM characterization by LC-OCD in a SWRO desalination line, Desalin. Water Treat., 51 (2013) 1776-1780.
[33] S. Jeong, S. Vigneswaran, Practical use of standard pore blocking index as an indicator of biofouling potential in seawater desalination, Desalination, 365 (2015) 8-14.
[34] S. Jeong, G. Naidu, S. Vigneswaran, C.H. Ma, S.A. Rice, A rapid bioluminescence-based test of assimilable organic carbon for seawater, Desalination, 317 (2013) 160-165.
[35] T.H. Chong, F.S. Wong, A.G. Fane, The effect of imposed flux on biofouling in reverse osmosis: Role of concentration polarisation and biofilm enhanced osmotic pressure phenomena, J. Membrane Sci., 325 (2008) 840-850.

543 [36] G. Naidu, S. Jeong, S. Vigneswaran, S.A. Rice, Microbial activity in biofilter used as a
544 pretreatment for seawater desalination, Desalination, 309 (2013) 254-260.
545 [37] S.R. Suwarno, X. Chen, T.H. Chong, D. McDougald, Y. Cohen, S.A. Rice, A.G. Fane,
546 Biofouling in reverse osmosis processes: The roles of flux, crossflow velocity and
547 concentration polarization in biofilm development, J. Membrane Sci., 467 (2014) 116-125.
548 [38] S. Park, M.H. Lee, J.S. Lee, T.K. Oh, J.H. Yoon, Thalassobius maritimus sp nov.,
549 isolated from seawater, Int. J. Syst. Evol. Micr., 62 (2012) 8-12.
550 [39] S.E. Langille, R.M. Weiner, Spatial and temporal deposition of Hyphomonas strain VP-6
551 capsules involved in biofilm formation, Appl. Environ. Microb., 64 (1998) 2906-2913.
552 [40] E.B.M. Denner, D. Vybiral, M. Koblizek, P. Kampfer, H.J. Busse, B. Velimirov,
553 Erythrobacter citreus sp nov., a yellow-pigmented bacterium that lacks bacteriochlorophyll a,
554 isolated from the western Mediterranean Sea, Int. J. Syst. Evol. Micr., 52 (2002) 1655-1661.
555 [41] M. Koblizek, O. Beja, R.R. Bidigare, S. Christensen, B. Benitez-Nelson, C. Vetriani,
556 M.K. Kolber, P.G. Falkowski, Z.S. Kolber, Isolation and characterization of Erythrobacter sp
557 strains from the upper ocean, Arch. Microbiol., 180 (2003) 327-338.

558

559

560

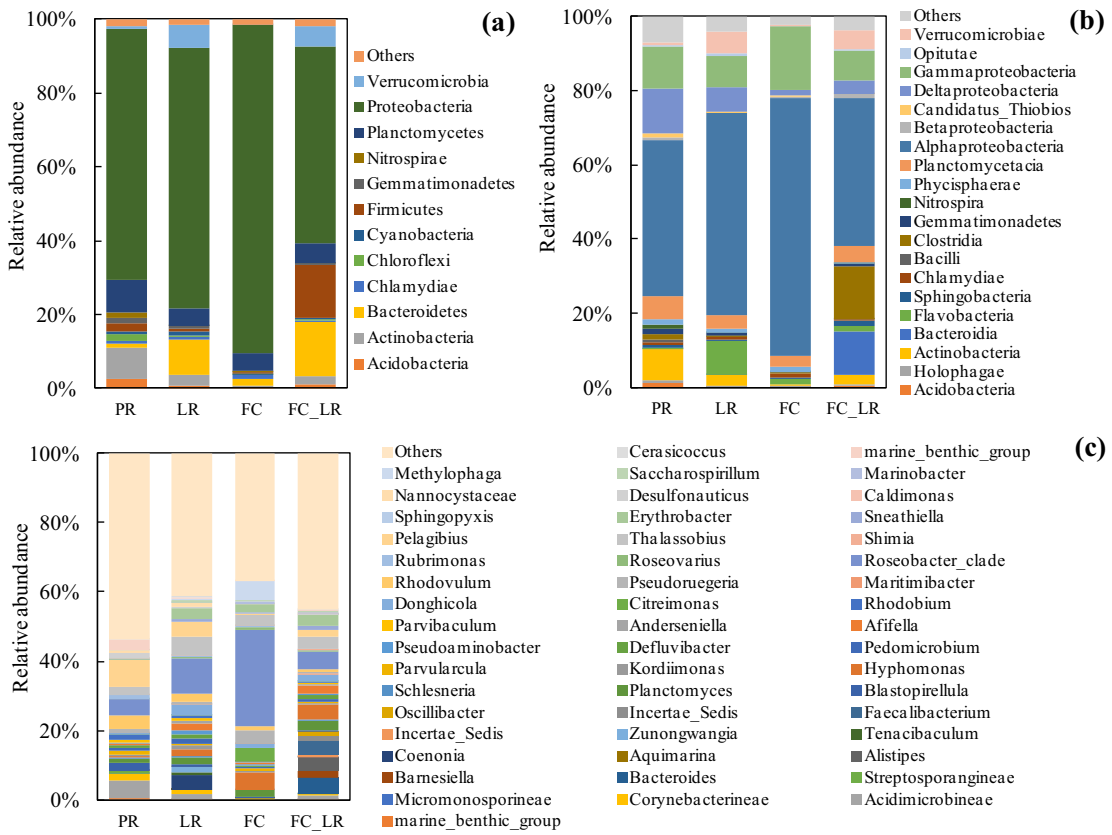

Figure 1. Prokaryotic community compositions in the membrane biofouling layers of GDM systems by sequencing at (a) the phylum level, (b) the class level, (c) the genus level. ‘‘Others” represents all classified taxa that were <1% and unclassified taxa. PR, LR, FC, and FC_LR are the abbreviations for pilot GDM reactor, lab GDM reactor, GDM filtration cell, and submerged filtration cell in the lab GDM reactor, respectively.

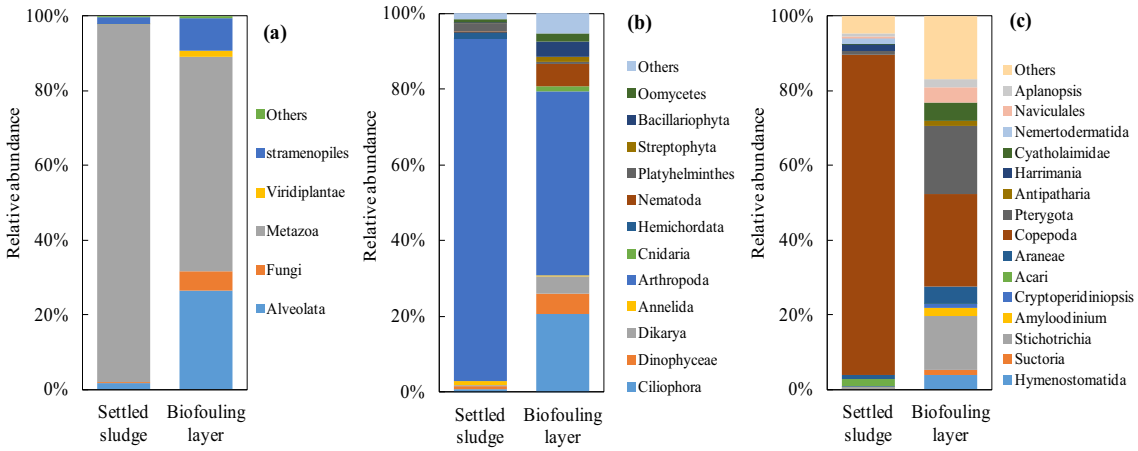

Figure 2. Eukaryotic community compositions of the settled sludge and biofouling layer of pilot GDM reactor by sequencing at (a) the phylum level, (b) the class level, (c) the genus level. ‘‘Others” represents all classified taxa that were <1% and unclassified taxa.

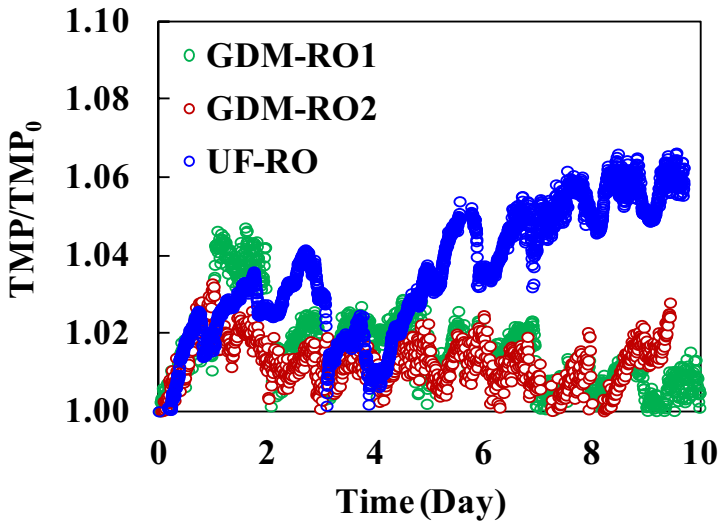

Figure 3. Effect of GDM and UF pretreatment on RO performance.

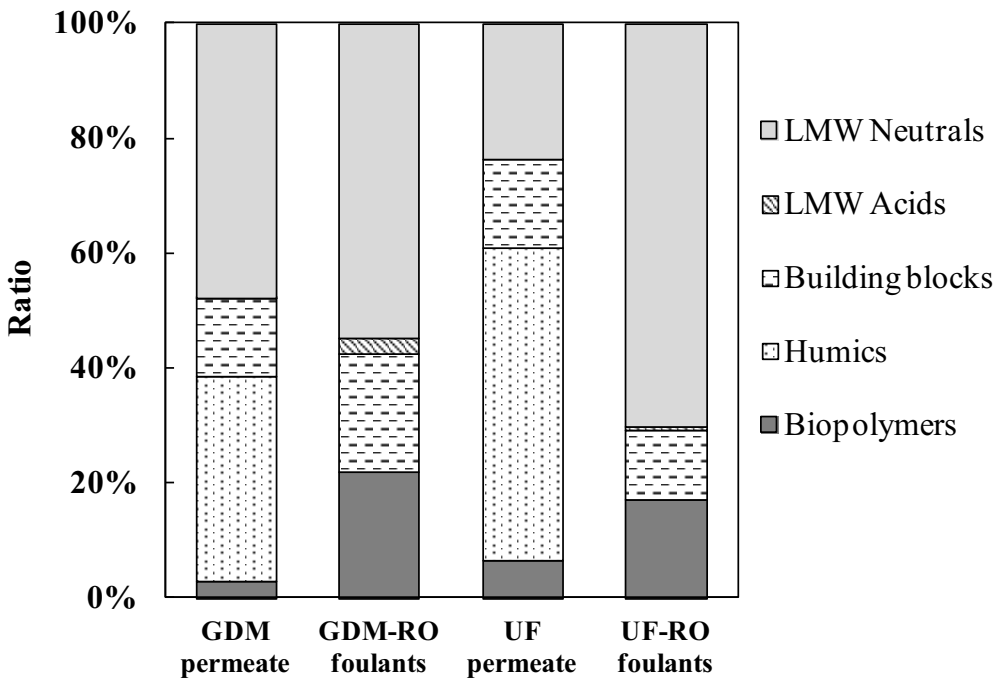

Figure 4. Contribution ratios of soluble organic substances in the RO feed waters and fouling layers.

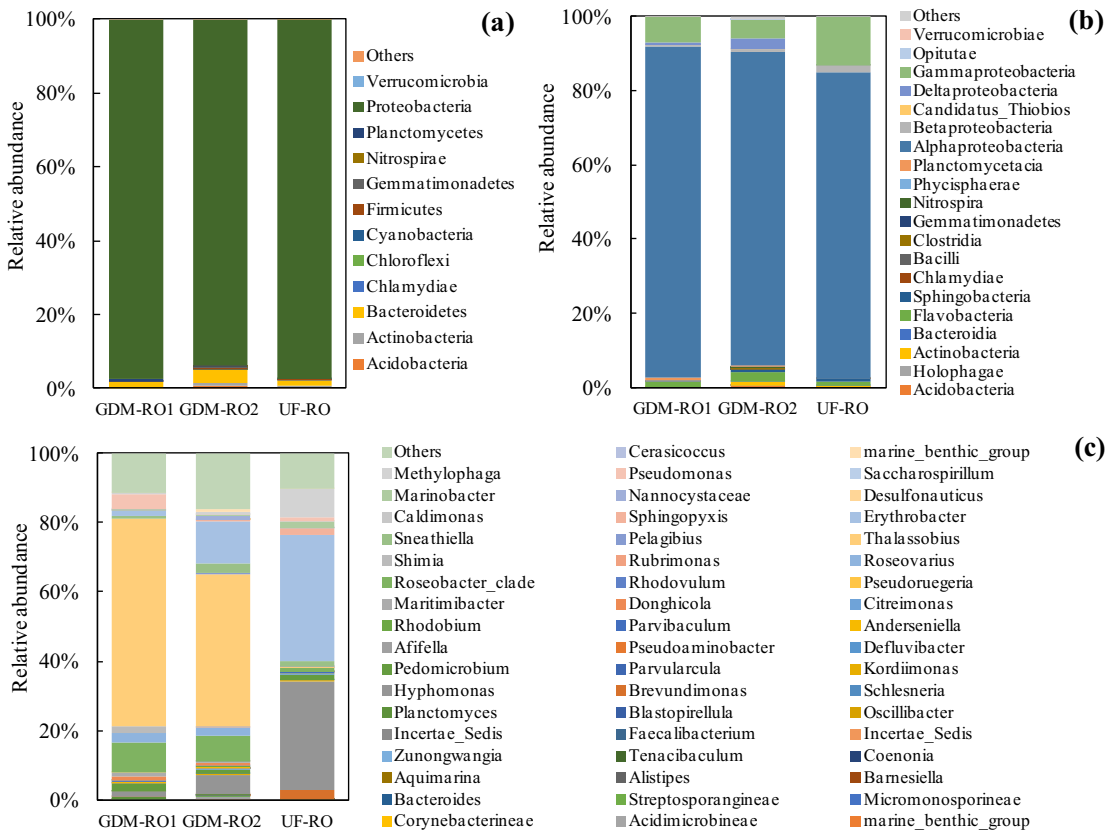

Figure 5. Prokaryotic community compositions in the biofouling layer on the RO membranes by sequencing at (a) the phylum level, (b) the class level, (c) the genus level. ‘‘Others” represents all classified taxa that were <1% and unclassified taxa.

Table 1. Characteristics of pilot GDM permeate [12] and full-scale UF permeate

Parameter	GDM permeate [12]	UF permeate
TEP (mg Gum Xanthan/L)	1.89±1.56	0.63±0.25
Bacterial count (10^4 Cell/mL)	0.28±0.16	0.31±0.26
DOC (mg/L)	1.29±0.33	1.21±0.13
Biopolymers (µg/L)	47 ±15	79±23
Humics (µg/L)	504±39	574±52
Building blocks (µg/L)	186±28	203±14
LMW neutrals (µg/L)	509±283	347±57
LMW acids (µg/L)	1±4	2±4
AOC (µg/L)	68±2	206±138

Table 2. Characteristics of RO foulants

Parameter	GDM-RO	UF-RO
ATP (ng/cm^2)	2.18±0.19	6.47±0.67
Biovolume (Live, 10^7 μm^3/cm^2)	2.65±0.19	6.70±0.99
Biovolume (Dead, 10^7 μm^3/cm^2)	0.58±0.14	3.14±2.32
DOC (μg/cm^2)	0.96±0.19	2.22±0.56
Biopolymers (μg/cm^2)	0.18±0.02	0.30±0.22
Humics (μg/cm^2)	N.D.*	N.D.
Building blocks (μg/cm^2)	0.17±0.02	0.21±0.03
LMW neutrals (μg/cm^2)	0.45±0.19	1.21±0.17
LMW acids (μg/cm^2)	0.02±0.02	0.01±0.01

*N.D. represents not detectable.

Supplementary data:

Table S1. A summary of GDM systems [1]

Parameter	Pilot GDM reactor	Lab GDM reactor	GDM filtration cell	GDM filtration cell submerged to lab reactor
Effective volume (L)	710	8.4	0.0046	0.0046
Averaged HRT (h)	21.6	13.0	0.74	13.0
Operation time (day)	250	45	45	25
Stabilized Permeate flux (L/m^2h)	18.6±1.4	16.3±0.2	2.7±0.6	17.2±0.8

Table S2. The characteristics of feed seawater [1]

Turbidity (NTU)	2.79±2.61
TEP (mg Gum Xanthan/L)	3.22±0.06
Bacterial amount (10^4 CFU)	4.78±0.86
DOC (mg/L)	1.08±0.16
AOC (µg/L) (n=4)	159±84
Biopolymers (µg/L)	69±15
Humic substances (µg/L)	522±61
Building blocks (µg/L)	172±12
LMW neutrals (µg/L)	309±149
LMW acids (µg/L)	0±0

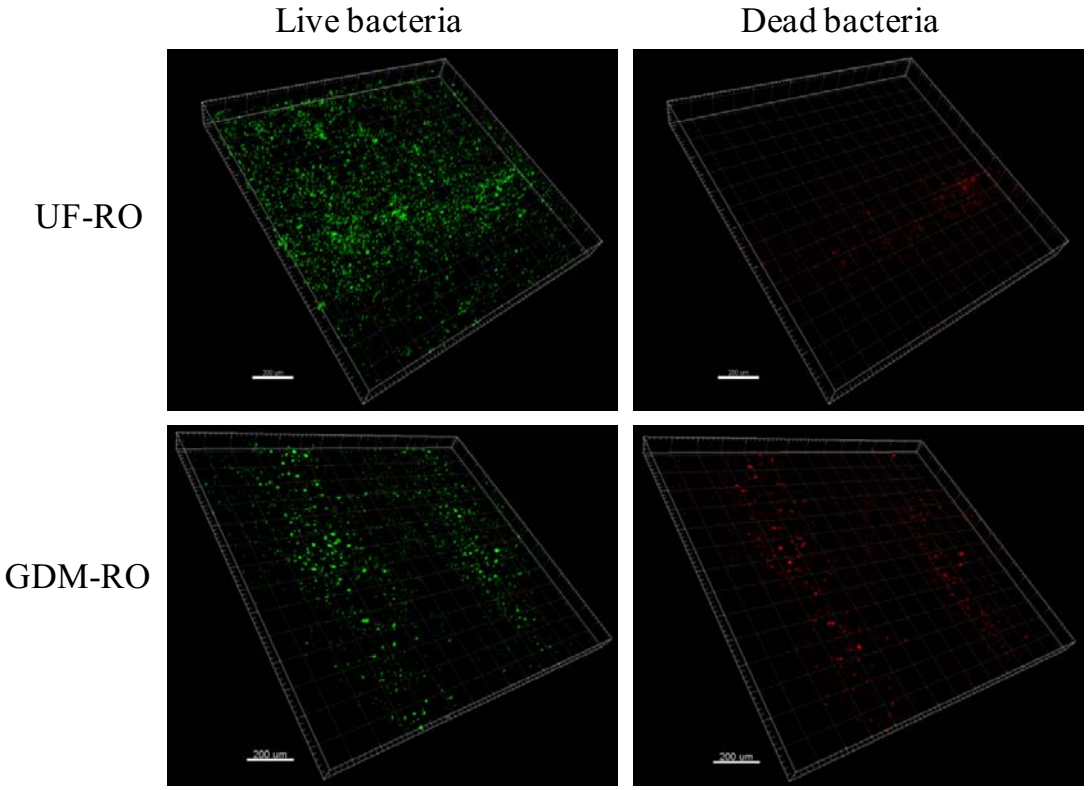

Figure S1: CLSM images of the biofilm on UF-RO and GDM-RO membranes.

Reference:

[1] B. Wu, T. Christen, H.S. Tan, F. Hochstrasser, S.R. Suwarno, X. Liu, T.H. Chong, M. Burkhardt, W. Pronk, A.G. Fane, Improved performance of Gravity-Driven Membrane Filtration for Seawater Pretreatment: Implications of Membrane Module Configuration, Water Res., 114 (2017) 59-68.

> GDM reactor dimension influenced dominant bacterial species in fouling layers.

> *Stichotrichia*, *Copepoda*, and *Pterygota* were dominant eukaryotes in the pilot GDM.

> GDM pretreatment led to lower RO fouling than UF system.

> GDM filtration produced a permeate with less amounts of AOC and biopolymers.

> Pretreatment affected dominant bacterial species on RO membranes.